Experimental Investigation of Free Convection in a Vertical Rod Bundle—A General Correlation for Nusselt Numbers

M. Keyhani
Department of Mechanical and Aerospace Engineering, The University of Tennessee, Knoxville, TN 37996-2210
Mem. ASME

F. A. Kulacki
Department of Mechanical and Aerospace Engineering, University of Delaware, Newark, DE 19716
Mem. ASME

R. N. Christensen
Department of Mechanical Engineering, The Ohio State University, Columbus, OH 43210

Free convection in two vertical, enclosed rod bundles has been experimentally investigated for a wide range of Rayleigh numbers. A uniform power dissipation per unit length is supplied to each rod, and the enclosing outer cylinder is maintained at constant temperature. Nusselt numbers for each rod, as well as an overall value for each bundle, have been obtained as a function of Rayleigh number. Comparison of the results for air and water as the working fluid indicate that, for a fixed Rayleigh number, an increase in the Prandtl number produces a reduction in the Nusselt number. This is contrary to what has been reported for vertical cavities and is attributed to curvature effects. Furthermore, the data reveal the interesting fact that it is quite possible for the individual rods in the bundle to exchange energy with the working fluid via different but coexisting regimes at a given power dissipation. Also, as the Rayleigh number is increased, the rods each tend to assume nearly the same heat transfer coefficient. Finally, a correlation for the overall convective Nusselt number is developed in terms of Rayleigh number and geometric parameters.

Introduction

Heat transfer measurements are presented for free convection in enclosed vertical rod bundles. Two rod bundles have been studied in the present work: a 3 × 3 array with $P/d = 3.08$, $L/d = 138$, and $L/D = 10.62$, and a 5 × 5 array with $P/d = 2.25$, $L/d = 92.42$, and $L/D = 5.79$. A uniform power dissipation per unit length in each rod is maintained, while the enclosing outer cylinder is held at constant temperature. The results include individual rod temperature distributions, heat transfer coefficients, and correlations for Nusselt numbers, all as a function of Rayleigh number and geometric parameters.

The plans for storage or disposal of spent fuel rod bundles from nuclear power reactors, encapsulated in air or helium-filled canisters, have led to a number of studies in this area. Previous studies on natural convection in rod bundles were concerned with temporary storage at the reactor site where the rod bundles are not enclosed [1]. In the case of an air or helium-filled canister containing the spent fuel rod bundle, the heat transfer problem becomes quite involved and difficult. The three modes of heat transfer, conduction, convection, and radiation, are superimposed. Moreover, the power dissipated by the rod bundle decays with time and is not uniform along the length of each rod.

Radiative heat transfer within an enclosed rod bundle has been studied by a number of investigators [2, 3, 4]. Also, some center rod temperature measurements of an actual spent fuel rod bundle, 15 × 15 rods with $P/d = 1.33$, enclosed in an air or helium-filled canister are available [5]. These temperature measurements are in good agreement with the predictions by a computer code, HYDRA-I, developed by McCann [6]. His code is programmed to treat transient three-dimensional coupled conduction, convection, and radiation in an enclosed rod bundle. The code provides a finite-difference solution in Cartesian coordinates to the continuity, momentum, and energy equations. In his study, the equation of motion is based on a generalization of flow through porous media, where the term for viscous forces is retained. The results obtained through the HYDRA-I code are temperature profiles of the rods in the array for different test fluids and boundary conditions on the canister surface. No parametric dependence of the heat transfer coefficient on the outer cylinder surface to flow parameter, Ra_D, or geometric factors is reported. Furthermore, the HYDRA-I code does not provide any information with respect to the relative contribution of convective heat transfer to the total energy transferred.

The main objective of the present study is to provide basic heat transfer data, convection Nusselt number as a function of Rayleigh number, in rod bundles where (*a*) coupled radiation, conduction, and convection heat transfer processes are present and (*b*) the pitch-to-diameter ratio, P/d, and the outer cylinder diameter are large enough so that porous media assumptions used in [6] are no longer valid.

Experimental Apparatus and Procedure

3 × 3 Rod Bundle. An existing outer cylinder with the associated controls and instrumentation [7] is used in the present study. The rod bundle that is placed in this canister consists of the top plate, nine heater rods, and the guide. The guide is 0.32-cm-thick Phenolite and is attached at the bottom of the rod bundle so that the desired pitch distance is maintained.

The top plate is carbon steel and is threaded for fastening with the cylinder, which is threaded internally. Nine holes of 0.64 cm diameter are drilled and tapped to accept the fittings at the top ends of the heater rods. These holes are on a square grid of 3.92 cm × 3.92 cm, which fits inside a circle of 8.26 diameter. The pitch distance between the holes is 1.95 cm.

Three 0.64-cm-dia holes on 3.22-cm centers are drilled and tapped in the top plate. Two Conax thermocouple connectors are fitted in these holes. The third hole is fitted by a Quick-Connect for the purpose of pressurizing or evacuating the system.

A square groove of 0.64 cm × 0.64 cm is cut into the lower surface of the top plate. The groove connects one of the holes

Contributed by the Heat Transfer Division for publication in the JOURNAL OF HEAT TRANSFER. Manuscript received by the Heat Transfer Division February 1, 1984. Paper No. 84-HT-72.

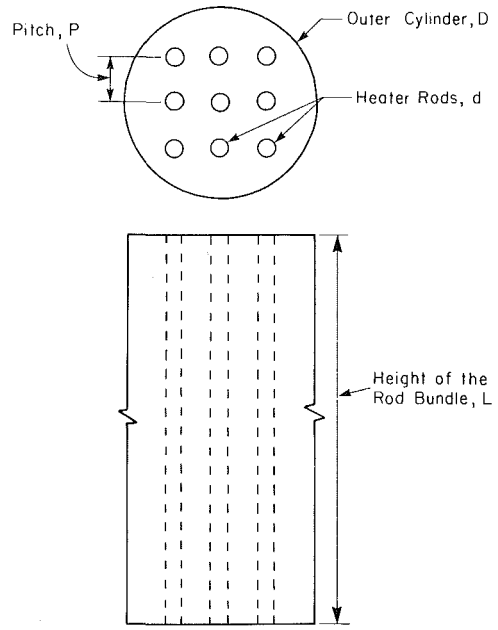

Fig. 1 Schematic of the enclosure and the assigned nomenclature for the length scales

for a Conax thermocouple connector to the hole for the center heater rod. This groove is used to channel the thermocouples close to the center rod. Then the thermocouples are lowered into the cylinder parallel to the heater rod. The thermocouples are affixed to the surface of the rod with plastic steel. The other rods in the bundle are instrumented in a similar manner.

The rod bundle comprises nine 0.635 cm dia × 91.44 cm cartridge heaters. The length includes a 1.27-cm-long threaded fitting at the top of the heater element. Each heater has an effective heated length of 87.6 cm and is designed to provide uniform electrical power dissipation per unit length. It comprises a nickel-chromium wire wound around a magnesium oxide core with a 0.05-cm Incoloy sheath.

The outer cylinder is of carbon steel and is 8.25 cm i.d. × 9.53 cm o.d. × 92.17 cm. To maintain it at constant temperature, 30.48 m of 0.9-cm-dia soft copper tubing is used to provide a cooling coil around the outer surface. This coil is wound in a counter flow manner to give a uniform surface temperature. A gap of 0.64 cm is provided between consecutive turns of the coil for emplacement of thermocouples along the surface. Figure 1 presents a schematic of the enclosure and the assigned nomenclature for the length scales.

5 × 5 Rod Bundle. The design of the apparatus for the 5 × 5 array is comprised of four major components: top plate, cylinder, and heated elements. In general, these components are configured similarly to those in the apparatus for the 3 × 3 array.

The top plate is a 2.54-cm-thick piece of brass with a 33.97-cm diameter. Twenty-five holes 1.91 cm in diameter are drilled and tapped in this plate for mounting the heating elements. These holes are located on a 21.44 cm × 21.44 cm square, which fits inside a circle of 30.31 cm diameter. The pitch distance between the holes is 4.29 cm. For introducing either air or another gas into the cylinder, a 0.63-cm-dia threaded hole on 13.28 cm center is drilled into the top plate. Four holes of 1.91-cm diameter on 12.86-cm centers are drilled and tapped in the top plate to accommodate four Conax thermocouple connectors.

The brass cylinder is 30.48 cm i.d. × 31.43 cm o.d. and 185.42 cm long. Two collars of 31.43 cm i.d. × 33.97 cm o.d. with a thickness of 1.27 cm are silver soldered to the top

Nomenclature

A_d = area of heater rod, m^2
A_D = area of outer cylinder, m^2
AR = height-to-diameter ratio of the cylinder or rod
C_p = specific heat at constant pressure, J/kg-K
d = diameter of a heater rod, m
d_i = diameter of equivalent inner cylinder, Nd, m
D = diameter of outer cylinder, m
g = gravitational constant, m/s^2
Gr = Grashof number, $g\beta l^3 \Delta T/\nu^2$
h_D = convective heat transfer coefficient on the inner cylinder, W/m^2
h_{di} = overall convective heat transfer coefficient on outer cylinder, $Q_c/A_D\Delta T$, W/m^2-K
h = convective heat transfer coefficient on the ith rod, $W_c/A_d(T_{MRi} - T_{MC})$, W/m^2-K
H = aspect ratio, L/l
k = thermal conductivity, W/m-K
K = radius ratio, r_o/r_i
l = annular gap, $r_o - r_i$, m
L = height of the cylinder or rod, m
N = number of rows in the square rod array
Nu = convective Nusselt number, hl/k
Nu_D = overall convective Nusselt number, $h_D D/k$
Nu_{di} = convective Nusselt number on ith rod, $h_{di}d/k$
P = center-to-center distance between the rods in a row, m
Pr = Prandtl number
q = convective heat flux based on the inner cylinder area, W/m^2
Q = total power input, W
r = radius, m
Ra = Rayleigh number, GrPr
Ra* = modified Rayleigh number, $\left(\frac{gB}{\alpha\nu}\right)\left(\frac{gl}{k}\right)l^3$
Ra_D = Rayleigh number based on diameter of outer cylinder, $(g\beta/\alpha\nu)D^3\Delta T$
Ra_{di} = Rayleigh number based on diameter of heater rod for rod i $(g\beta/\alpha\nu)(T_{MRi} - T_{MC})d^3$
T = temperature, K
ΔT = characteristic temperature difference, $T_{MR} - T_{MC}$, °C, for rod bundles T_{MR} is evaluated on the center rod
W = power per rod, W
W_c = energy transferred by convection for a given heater rod, W
y = coordinate measuring distance along rod from bottom, m
α = thermal diffusivity, $k/\rho C_p$, m^2s
β = isobaric coefficient of thermal expansion, K^{-1}
ϵ = emissivity
ν = kinematic viscosity, m^2/s
ρ = density, kg/m^3
σ = Stefan-Boltzmann constant, 5.669×10^{-8}, W/m^2-K^4

Subscripts

c = convection
d = based on rod
D = based on outer cylinder
i = inner
MC = mean value on outer cylinder
MR = mean value on rod
o = outer
R = rod

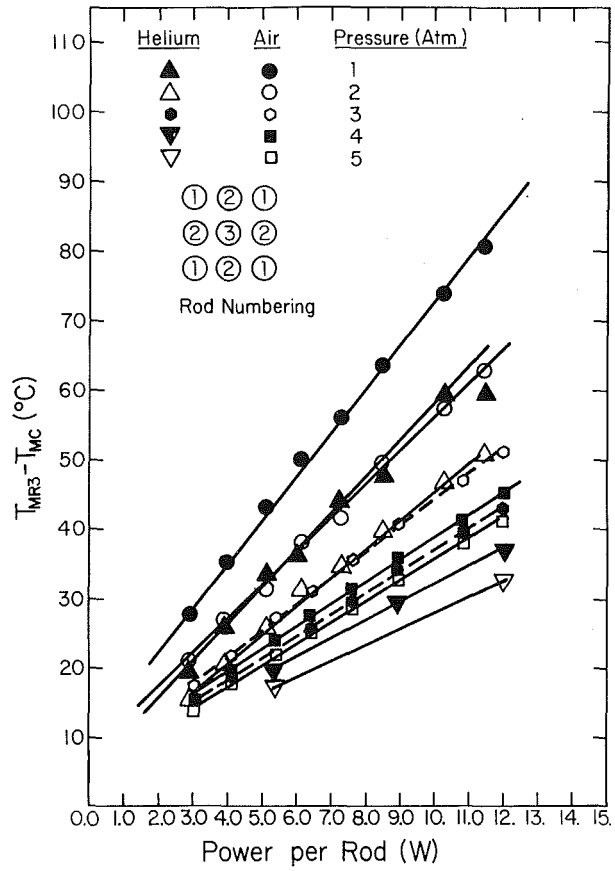

Fig. 2 Average temperature difference on center rod $T_{MR3} - T_{MC}$ as a function of total power per rod

and bottom ends of the cylinder. Sixteen equally spaced holes of 0.95-cm diameter on 16.75-cm centers are drilled through the end plates and collars. These holes facilitate the bolting of the end plates to the cylinder. Also, two separate soft copper cooling coils of 0.95-cm diameter are soft soldered to the top and bottom half of the cylinder. This coil will be used for circulating water to maintain the cylinder wall at constant temperature. Forty-eight holes of 0.13-cm diameter are drilled along the length of the cylinder. These holes are located along four lines, twelve holes per line, that divide the cylinder into four equal parts. Surface temperature thermocouples are placed in these holes.

The rod bundle comprises twenty-five 1.91-cm-dia cartridge heaters with an effective heated length of 176.5 cm. The basic design of the heater elements is similar to those used in the 3 × 3 rod bundle. A 30-cm-dia × 1.27-cm-thick Phenolite guide with twenty-five holes of 1.91-cm diameter on a square grid the same as the top plate is attached to the bottom of the rods to maintain the square array. Thermocouples are attached to the rods in this array in a manner similar to that for the 3 × 3 rod bundle.

Measurements of rod temperatures are made to within 0.1°C to 0.2°C using a variety of recording data loggers and voltmeters. Power to the heated rods is supplied through a filtered voltage regulator and transformers. Power to each rod in the bundle is held to within 1 percent of the set value under normal conditions for free convection. The radiation correction for each rod, however, requires that power input be adjusted to produce a predetermined mean rod temperature. This was done manually after the system had been allowed to reach steady state under a vacuum. Normally, a data run for a rod bundle required from several days to three weeks owing to the time required to reach steady state and the trial-and-error procedure needed to obtain the radiative correction. A more detailed description of the experimental apparatus, instrumentation and procedure are given in [8, 9].

Results and Discussions

3 × 3 Rod Bundle

Air and Helium. Heat transfer data obtained from these experiments include total and convective Nusselt number for each rod as well as an overall value for the bundle for a wide range of Rayleigh number. The characteristic length used in the definition of overall Nusselt and Rayleigh numbers is the diameter of the outer cylinder. The temperature difference is taken as the difference between the average value of the center rod and that of the outer cylinder. The heat transfer coefficient is based on the area of the outer cylinder. In terms of overall Rayleigh number, heat transfer data cover the range of $1.95 \times 10^4 \leq \mathrm{Ra}_D \leq 4.5 \times 10^7$. This range covers the conduction to boundary layer flow regimes. The numbering of rods in the bundle is given in Fig. 2.

Seventy runs with air and helium at various pressures and power inputs to the rods were conducted. The characteristic temperature difference for the rod bundle, $T_{MR3} - T_{MC}$, is plotted as a function of power input to the rods in Fig. 2. For a given test gas and power input, an increase in the pressure corresponds to an increase in the Grashof number; consequently, a lower temperature difference is observed. Furthermore, for a given test gas and pressure, the dependence of the temperature difference on the variation in the power input is qualitatively indicative of the flow regime encountered. It should be noted that these temperature differences are a result of superimposed processes of conduction, convection, and radiation heat transfer. The following comparison of two data points is a good example of the interdependent effects of these processes. With air at a pressure of 5 atm, a temperature difference $T_{MR3} - T_{MC}$ of 22.42°C is obtained for a power input of 4.99 W/rod. In comparison, under a vacuum (a pressure of 9.2×10^{-5} atm), a temperature difference of 86.37°C is observed for the same power input. These data points correspond, respectively, to a convection-dominated heat transfer process to one in which radiation is the primary means of energy transfer.

Owing to the symmetry of the rod bundle, temperature measurements on only three rods in the square array are needed. In order to minimize the disturbance of the flow field, temperatures on Rods 1 and 2 are measured only at three locations (y/L = 0.25, 0.50, 0.75), whereas the temperature distribution on the center rod is measured on seven locations, starting at y/L = 0.125 with 0.125 intervals. For about 5 W/rod, temperature profiles on the rods with air, helium, water, and a vacuum are graphically presented in Fig. 3.

In the conduction regime, with helium as the convective medium, temperature distributions on the rods are nearly uniform. As the Rayleigh number is increased to 1.77×10^6, with air as the test gas, temperature profiles show a steady increase from the leading edge to the top of the heaters. This is particularly evident from the data on the center rod, for which temperatures are measured at seven locations.

With air and helium as the convective media, at the same axial location, the center rod, Rod 3, has the highest temperature compared to those for Rods 2 and 1. This difference between the temperatures on the rods is more pronounced in the conduction regime. Although the presence of radiation heat transfer results in a variation in the temperatures of rods, it is not the only factor. Consider the enclosure filled with fluid such that thermal radiation is not present. In the conduction regime, and with the same power input to each rod, one would expect the lowest mean temperature on the rod closest to the outer cylinder, and the highest on the center rod. Thereafter, as the Grashof number is increased, upward flows

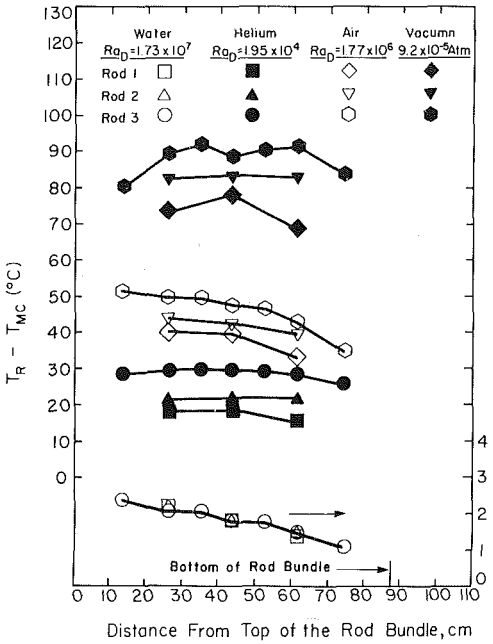

Fig. 3 Local temperature difference on Rods 1, 2, and 3 for various Rayleigh numbers

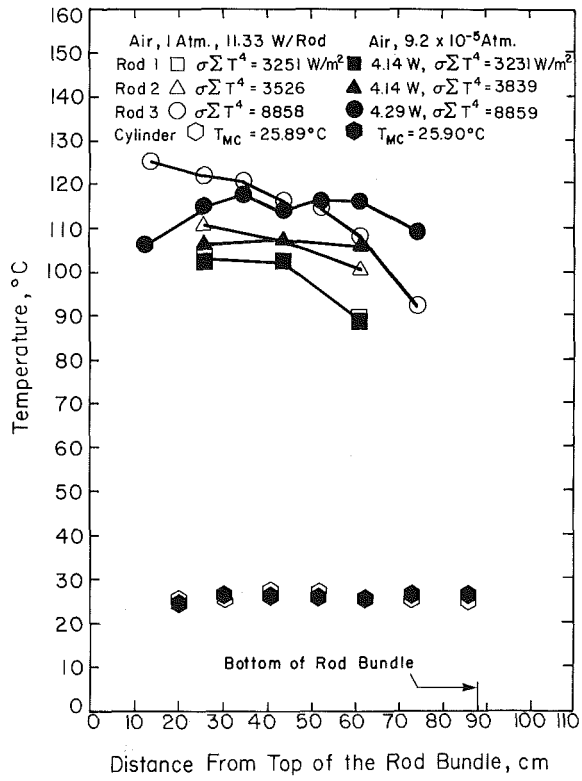

Fig. 4 Temperature distributions in the 3 × 3 rod bundle under vacuum conditions

are initiated around the individual rods. Each rod will have a distinct temperature profile which depends on its position in the bundle. Quantitatively, air and helium temperature data support this explanation.

This explanation, however, is not supported by the water data, as can be seen from Fig. 3; the temperature profiles on Rods 1, 2, and 3 are nearly the same. One possible reason is that, in the boundary layer regime in a vertical enclosure, the Nusselt number (with the height of the enclosure as the length scale) shows a weak or nonexistent dependence on the height-to-gap width ratio [10–13]. Extending this observation to the present case, one can state that, in the boundary layer regime, the distance of a given rod in the bundle to the outer cylinder has no effect on the heat transfer coefficient for that rod. It should also be mentioned that for same Rayleigh number range, flow regimes for water ($Pr > 1$) and air ($Pr < 1$) do not necessarily correspond.

Temperature distributions on Rods 1, 2, and 3 for a power input of 5.0 W/rod at a pressure of 9.2×10^{-5} atm are also given in Fig. 3. At this pressure, radiation is the predominant mode of heat transfer, but conduction effects are not totally eliminated. As discussed earlier, both of these modes of heat transfer have a strong effect on the extent of temperature variations from one rod to another. This is due to exposure and distance of various rods to the outer cylinder (see Fig. 1).

In order to obtain convective heat transfer coefficients the following procedure is followed. For a given gas and power input per rod, mean temperatures on Rods 1, 2, and 3 are obtained. The cavity is then evacuated, and the outer cylinder temperature is maintained the same as when the gas is present. The power inputs to Rods 1, 2, and 3 are simultaneously adjusted until the mean temperatures on these rods are the same as those obtained with the convection present. These power inputs are considered to be the radiation contribution augmenting the heat transfer process when the gas is present. At the vacuum condition, the Rayleigh number Ra_D is about 0.02, which is well below the value obtained for conduction regime ($Ra_D = 1.3 \times 10^4$). Nevertheless, at this low Rayleigh number, some energy is still transferred by conduction. This conduction effect is estimated [8] and is included in the uncertainty in the Nusselt number.

Temperature distributions obtained from a typical experiment under a vacuum are plotted in Fig. 4. Superimposed on these temperatures are the profiles observed with convective heat transfer present. Under vacuum conditions, the average temperatures on the individual rods and the outer cylinder are reproduced to within 0.9 percent of the values observed with the convective effects present. Although the temperature profiles on the rods under vacuum conditions are different from those observed with convection present, the calculated values of the parameter $\Sigma\sigma T^4$ (emissive power) for the individual rods are nearly the same for the two conditions. Therefore, it is felt that the radiation heat transfer contributions are adequately accounted for.

The radiation heat transfer contributions for Rods 1, 2, and 3 vary with the test gas and the Rayleigh number. In the conduction regime, with helium as the convective medium, the radiation contributions as percentages of the power input per rod, for Rods 1, 2, and 3 are approximately 15, 16, and 26 percent, respectively. At $Ra_D = 5.81 \times 10^5$, the corresponding values are 11.4, 11.9, and 14.1 percent. With air at 1 atm, $Ra_D = 1.77 \times 10^6$, the radiation contributions for Rods 1, 2, and 3 are about 37, 37, and 42 percent of the total Nusselt numbers, respectively, whereas at 5 atm, $Ra_D = 4.47 \times 10^7$, the corresponding values are reduced to about 16, 16, and 18 percent.

Convective Nusselt numbers Nu_d for Rods 1, 2, and 3 are graphically presented as a function of Rayleigh number Ra_d in Fig. 5. The characteristic length used in the definition of Ra_d and Nu_d is the rod diameter. The temperature difference is taken as the difference between the average values on the given rod and that of the outer cylinder. The heat transfer coefficient is defined based on the rod area. All the thermophysical properties are evaluated at the mean value of temperatures of the given rod and that of the outer cylinder.

The individual rods in the bundle, under a given condition of uniform power input per rod, can exchange energy with the working fluid via different but coexisting flow regimes. At $Ra_d = 44.8$ the Nusselt number for Rod 1 is 10 percent higher than its asymptotic conduction value and can be classified as

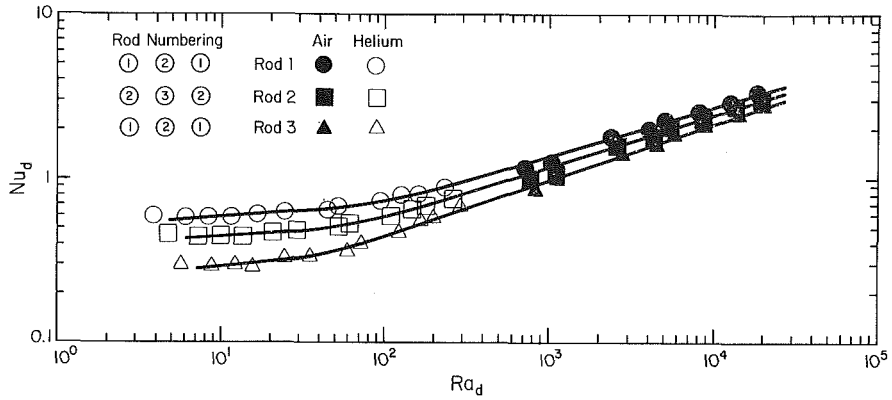

Fig. 5 Average convective Nusselt numbers for the individual rods in the 3 × 3 rod bundle

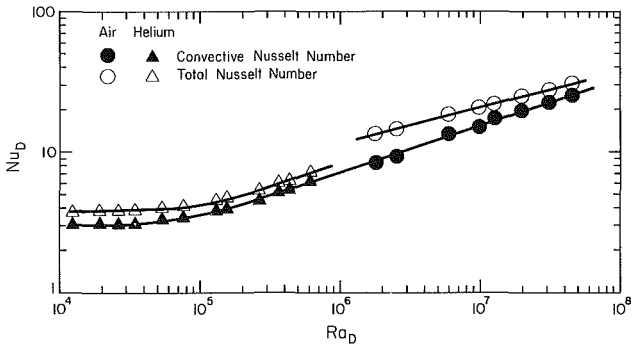

Fig. 6 Overall convective Nusselt numbers for the 3 × 3 rod bundle

being in the conduction flow regime (see flow regime classification given in [13]). Under the same conditions, Rod 3 is at $Ra_d = 59.7$ and the Nusselt number is 26 percent higher than its asymptotic conduction value. Hence, under a given condition, Rod 1 is in conduction flow regime while Rod 3 is in transition flow regime.

The fact that the conduction flow regime ends at a lower Rayleigh number for Rod 3 than for Rods 1 and 2 should not be unexpected. In a vertical cavity or annulus, the Rayleigh number at which conduction regime ends is proportional to the aspect ratio, where the aspect ratio is defined as the ratio of the height of the layer to distance between cold and hot surfaces [10, 13]. In the 3 × 3 rod bundle, the height of the heated surface is the same for Rods 1, 2, and 3, but the characteristic distance between the hot and cold surfaces is a maximum for the center rod, and a minimum for Rod 1. Therefore, if a characteristic aspect ratio is to be defined for the rods in the bundle, highest and lowest characteristic aspect ratios would be assigned to Rods 1 and 3, respectively.

As can be seen from Fig. 5, Rod 1 has the highest convective Nusselt number, which is a direct consequence of proximity to the outer cylinder. The center rod, farthest from the outer cylinder, has the lowest heat transfer coefficient. The difference between the convective Nusselt numbers of the three rods is more pronounced in the conduction regime. However, it seems that with increase in Ra_d the Nusselt numbers for the three rods are converging.

The experimental data are correlated for the conduction and boundary layer regimes. The convective Nusselt numbers as a function of Rayleigh number for the individual rods in the array are as follows:

Rod 1

$$Nu_{d1} = 0.472Ra_{d1}^{0.086},\ 6 \le Ra_{d1} \le 1.3 \times 10^2 \quad (1)$$

$$Nu_{d1} = 0.159Ra_{d1}^{0.307},\ 1.3 \times 10^2 \le Ra_{d1} \le 1.84 \times 10^4 \quad (2)$$

Rod 2

$$Nu_{d2} = 0.347Ra_{d2}^{0.097},\ 7 \le Ra_{d2} \le 90 \quad (3)$$

$$Nu_{d2} = 0.126Ra_{d2}^{0.321},\ 90 \le Ra_{d2} \le 1.93 \times 10^4 \quad (4)$$

Rod 3

$$Nu_{d3} = 0.218Ra_{d3}^{0.124},\ 8 \le Ra_{d3} \le 50 \quad (5)$$

$$Nu_{d3} = 0.093Ra_{d3}^{0.341},\ 50 \le Ra_{d3} \le 2.04 \times 10^4. \quad (6)$$

The above correlations describe over 90 percent of the experimental data to within 5 percent, and the maximum deviation does not exceed 8.5 percent.

Overall convection and total Nusselt numbers as a function of Rayleigh number are graphically presented in Fig. 6. With air or helium, as the Rayleigh number is increased the radiation heat transfer contribution decreases. For air, radiation heat transfer accounts for 17–38 percent of the total power input, whereas with helium the radiative heat transfer is reduced to 13–19 percent of the total Nusselt number. The correlations for the convective Nusselt number as a function of Rayleigh number in conduction and boundary layer flow regimes are

$$Nu_D = 1.27Ra_D^{0.087},\ 1.95 \times 10^4 \le Ra_D \le 1.2 \times 10^5, \quad (7)$$

$$Nu_D = 0.072Ra_D^{0.332},\ 1.2 \times 10^5 \le Ra_D \le 4.5 \times 10^7. \quad (8)$$

The above correlations describe the experimental convective Nusselt numbers with a maximum deviation of 6 percent.

The experimental errors due to uncertainty in the measured quantities and thermophysical properties are about 5 and 6 percent for the Nusselt and Rayleigh numbers, respectively. However, the convective heat loss from the top plate, the axial conduction loss along the rods, which are partially accounted for in the radiation corrections, and the conduction heat transfer present in the vacuum experiments add to the uncertainty in the convective Nusselt number. A detailed analysis of the effects discussed above [8] indicates that 90 percent of the overall Nusselt numbers are underestimated by about 3.2 percent or less, with the maximum deviation not exceeding 7.1 percent for all the data points. Considering the complex geometry of the problem, however, it is felt that the reported uncertainties are satisfactory.

Water. The objective of these experiments is to provide baseline values for the convective Nusselt number. The air and helium results, with the appropriate Prandtl number effect taken into account, should be in agreement with those obtained with water. Otherwise, one can conclude that the radiation heat transfer effects are not adequately accounted for. A total of ten experimental runs with the power input to the heater rods varying from 2.38 to 35.8 W/rod were conducted. The Grashof number range covered is $1 \times 10^6 \le Gr_D \le 3.2 \times 10^7$. In some of the experiments, the Grashof number is increased by increasing the cylinder temperature

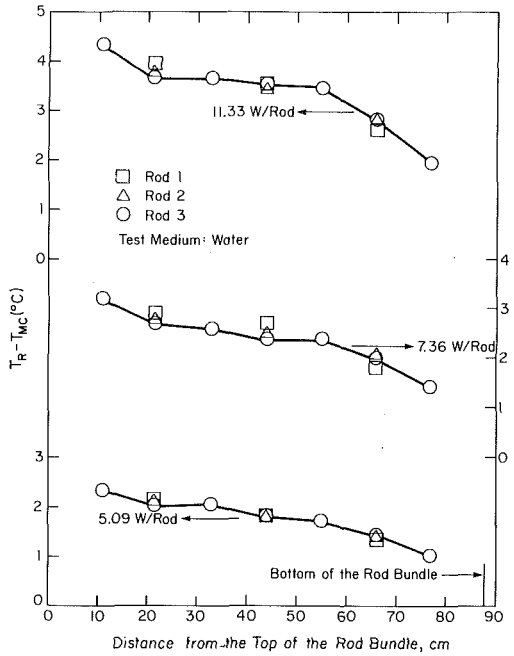

Fig. 7 Local temperature difference on Rods 1, 2, and 3 for various power inputs per rod (for water)

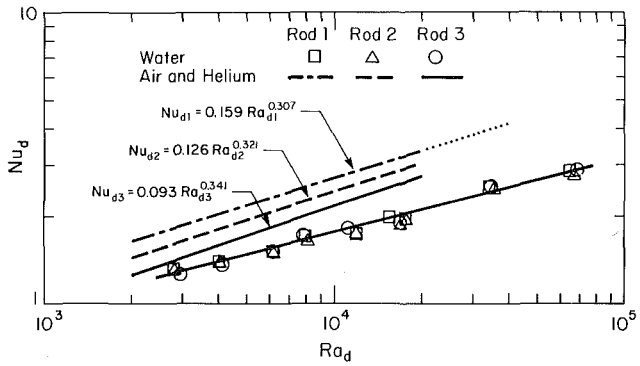

Fig. 8 Average Nusselt numbers for the individual rods in the 3 × 3 rod bundle (water results)

rather than the power input, i.e., raising the mean fluid temperature and as a result the value of the product of properties included in the Grashof number.

Temperature profiles on Rods 1, 2, and 3 for three experimental runs are given in Fig. 7. As mentioned earlier, the temperature profiles on the rods are nearly the same. One possible explanation for this behavior was offered, and will not be discussed further. The point which merits attention, however, is a discussion of the angular dependence of the temperature. The thermocouples on Rod 3 are facing Rod 1. As can be seen from Fig. 7, the measured temperatures, for a given axial location, regardless of their angular and radial positions, are nearly the same. This observation can be very helpful in analytical modeling of the problem. With the above observation in mind, one can state that, with air or helium as the test gas, at a given location the temperature of any rod in the bundle would exhibit a small variation along its periphery. Clearly, the extent of this variation is dependent on the degree of the exposure of the given rod to hot and cold surfaces.

Nusselt numbers for the individual rods in the array Nu_d are plotted as a function of Rayleigh number Ra_d in Fig. 8. The correlations obtained for the convective Nusselt number for Rods 1, 2, and 3 with the air and helium experiments are also graphically presented in this figure. The water results indicate that for a given Ra_d, the heat transfer coefficient is the same for the three rods. In comparison, as discussed

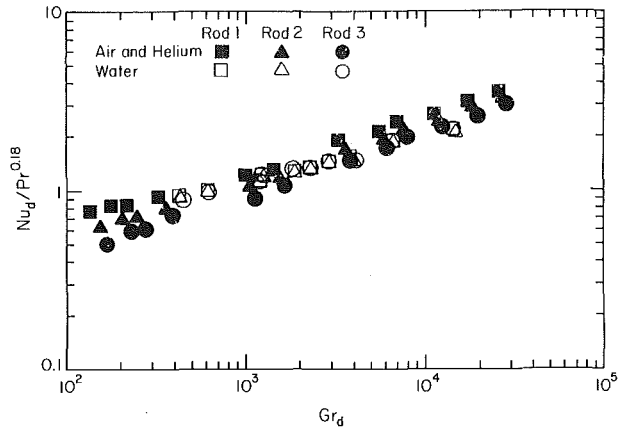

Fig. 9 Normalized Nusselt numbers for the individual rods in the 3 × 3 rod bundle $Nu_d/Pr^{0.18}$ as a function of Gr_d

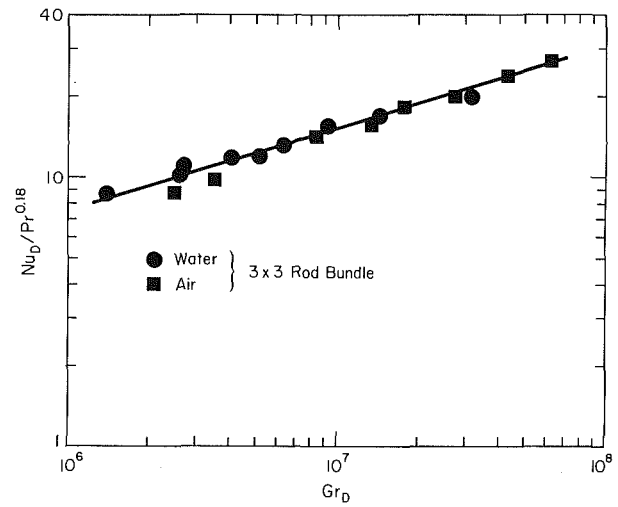

Fig. 10 Normalized overall Nusselt numbers for air and water as a function of Gr_D

earlier, there is a distinct difference in the convective Nusselt numbers of Rods 1, 2, and 3 when air or helium is the convective medium. As can be seen from the figure, the air and helium results, for a given Ra_d, yield a higher Nusselt number compared to that obtained from water experiments. This is contrary to the expected Prandtl number effect as reported for vertical cavities [11, 14] and annular enclosures [13]. However, a recent analytical and experimental study by Kubair and Simha [12] on free convection in annular enclosures reports a similar behavior to that found here. Their analytical results indicate that a correlation of Nusselt number as a function of Grashof and Prandtl numbers leads to a 0.18 exponent for the latter. Prandtl number range in their study was $0.01 \leq Pr \leq 5.0$. The results of their experiments with mercury and water confirmed their analytical findings. Moreover, this Prandtl number effect is confirmed through favorable agreement of the air and helium results reported in [7] with the water data obtained with the same annulus [8].

In order to find a reason for the possible difference between the Prandtl number effect in a vertical cavity as opposed to an annulus, one should concentrate on the studies on free convection about a vertical cylinder. However, none of the existing studies on this subject give an explicit Prandtl number effect on heat transfer. Nevertheless, the information given by Sparrow and Gregg [15], qualitatively, can be of help. Their analysis indicates that, for a fixed local Grashof number, a decrease in the Prandtl number results in a higher value for the ratio of the local heat transfer coefficient of the cylinder to that of a flat plate. Therefore, implicitly one can conclude that enhancement of the heat transfer coefficient due to

curvature effects becomes more pronounced as the Prandtl number is reduced. It should be mentioned that only two Prandtl numbers, 0.72 and 1.0, were considered by Sparrow and Gregg.

Assuming the same Prandtl number effect holds for the present case, the normalized Nusselt numbers $Nu_d/Pr^{0.18}$ for the individual rods and those for the rod bundle as a whole $Nu_D/Pr^{0.18}$, obtained with air, helium, and water are presented as a function of their respective Grashof number in Figs. 9 and 10, respectively. The water data for the individual rods, as can be seen from Fig. 9, are bracketed with those obtained with air and helium for Rods 1, 2, and 3. Considering the fact that air and helium results are different for each rod, and the water data are nearly the same for Rods 1, 2, and 3, it seems that a Prandtl number effect of $Pr^{0.18}$ is also adequate for the present case. Moreover, normalized overall convective Nusselt numbers obtained from air and helium experiments are in good agreement with those for water (see Fig. 10). Therefore, it is felt that air and helium data are properly corrected for the radiation effects.

The experimental water Nusselt numbers Nu_d for the individual rods in the array can be correlated in terms of Rayleigh number Ra_d with a maximum deviation of 6 percent. However, a single correlation can describe all the data obtained for the three rods to within 8 percent. Therefore, it is felt that a single correlation as

$$Nu_d = 0.162 Ra_d^{0.257}, \quad 2.8 \times 10^3 \le Ra_d \le 6.8 \times 10^4, \qquad (9)$$

is adequate.

The overall water Nusselt numbers for the rod bundle can be correlated in terms of Rayleigh number as

$$Nu_D = 0.151 Ra_D^{0.274}, \quad 6.5 \times 10^6 \le Ra_D \le 1.4 \times 10^8. \qquad (10)$$

Equation (10) describes the experimental data with a maximum deviation of 7 percent. The total uncertainties in the calculation of the Nusselt and Rayleigh numbers for the water experiments are estimated to be about 7 and 8 percent, respectively.

Flow Visualization. For these experiments, the 3 × 3 rod bundle assembly is placed inside a transparent acrylic cylinder of 7.46 cm i.d. The height-to-diameter ratio is 11.81. The aspect ratio AR of the outer cylinder in the heat transfer experiments was 10.61. The somewhat larger AR value for the acrylic cylinder is not expected to affect the flow field significantly. Ethylene glycol with suspended aluminum particles (5 to 50 μ) is used as the working medium. Illumination of the particles is done with a high-intensity lamp shining through a narrow slit so as to produce a plane of light.

Prior to flow visualization experiments, the bundle and the outer cylinder are calibrated with thermocouples in place. The thermocouples were then removed and a few grams of aluminum powder were poured into the cylinder. The system was allowed to reach steady state prior to illumination with the light source.

Results reported here are for $Ra_D = 2.92 \times 10^7$, $Ra_d = 1.83 \times 10^4$, and $Pr = 46.4$. (It should be noted that the rod Rayleigh number Ra_d is the same for Rods 1, 2, and 3 because the temperature field is nearly same for these rods.) The flow fields in the bottom, above midheight, and the top of bundle are given in Fig. 11. These photographs were taken with an exposure time of 20 to 60 s. The scale to the right in each

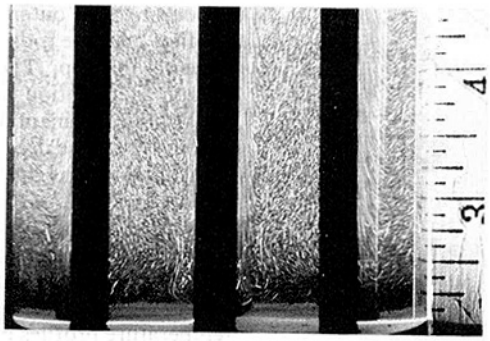

Fig. 11(a)

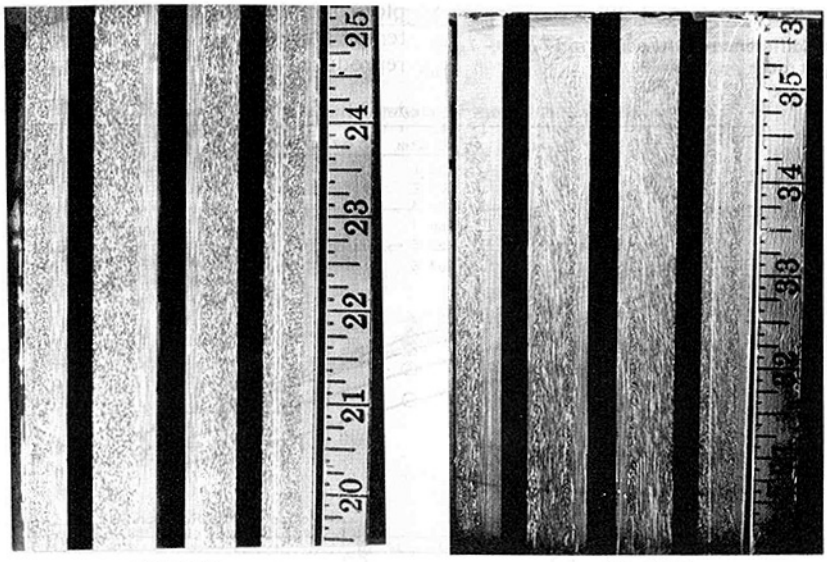

Fig. 11(b) Fig. 11(c)

Fig. 11 Flow field in the 3 × 3 rod bundle for $Ra_d = 1.83 \times 10^4$ and Pr = 46.4: (a) $0 \le y/L \le 0.07$, (b) $0.51 \le y/L \le 0.67$, (c) $0.81 \le y/L \le 1.0$

photograph is in inches, with the bottom of the bundle at 2 in. and the top at 36 in. One should keep in mind that these photographs were taken at an angle slightly off perpendicular to the plane of the light so one can see beyond the front row of rods facing the camera.

The major results of the flow visualization are that there is no interaction between the upward flow around adjacent rods. Except for the end regions, less than 5 cm from the ends, the upward flow around the rods has a uniform thickness. An unexpected finding is that there is a low-speed downward flow between the rods. This may be a result of the rather large P/d of this particular bundle (P/d = 3.08). This downward flow between the rods, in conjunction with the upward flow around the center rod and the cross flow at the end regions, results in vortex rings around the center rod in the end regions. In Fig. 11(*c*), one can see the traces of downward flow. Flow next to the outer cylinder can only be seen on the right-hand side of the graph next to the scale.

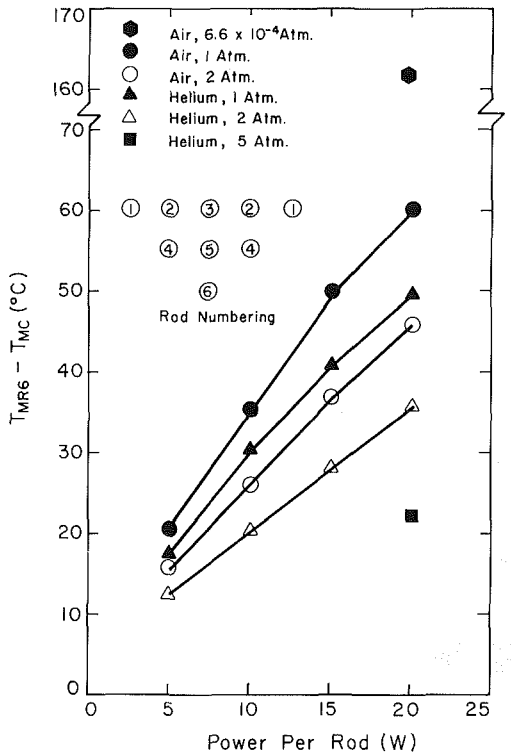

Fig. 12 Average temperature difference on the center rod $T_{MR6} - T_{MC}$ as a function of total power per rod

5 × 5 Rod Bundle. Total and convective heat transfer coefficients for each rod in the array as well as an overall value for the bundle are obtained for a wide range of Rayleigh number. Although Rayleigh number Ra_D was varied from 2.6×10^5 to 1.06×10^9, the conduction flow regime was not encountered. With helium at atmospheric pressure as the convective medium, the heat transfer results of the 3 × 3 rod bundle experiments were indicative of conduction flow regime. However, in the present case, the results obtained with helium at atmospheric pressure are indicative of the boundary layer flow regime.

The characteristic temperature difference for the rod bundle $T_{MR6} - T_{MC}$ as a function of power input to the rods for air and helium at various pressures is plotted in Fig. 12. The rod numbering is also given in that figure. The numbering of the rods is done in such a way that the rod closest to the outer cylinder, i.e., the rod on the corner of the square array, is numbered 1, and the center rod is number 6. A qualitative discussion of the temperature in this figure is similar to that given for Fig. 2.

Typical temperature profiles on Rods 1 to 6 obtained with air at 2 atm, $Ra_D = 3.83 \times 10^8$, are plotted in Fig. 13. There are several points about these temperature profiles which should be noted. The interior rods, i.e., Rods 4, 5, and 6, have nearly the same profile. Furthermore, Rods 2 and 3 also share the same temperature profile. Rod 1, closest to the outer cylinder and with most exposure to it, experiences the lowest temperature in the bundle. For this experimental run, the mean temperatures on Rods 1 to 6 are, respectively, 63.92°C, 67.4°C, 66.94°C, 69.78°C, 70.0°C, and 70.17°C. As the mean temperatures indicate, Rods 4, 5, and 6 are surrounded by high-temperature surfaces. Also, these rods have little exposure to the outer cylinder. Furthermore, the temperature profiles on these rods show a steady increase from the leading edge to the top. Therefore, it can be concluded that the combined radiation and conduction heat transfer processes are not the dominant mode of heat transfer from these rods.

The procedure used for the correction of the radiation heat transfer effects is the same as that followed in the 3 × 3 rod bundle experiments. Temperature distributions on Rods 1 and 6 obtained from a typical experiment in vacuum condition, at a pressure of 6.6×10^{-4} atm with Ra_D = 22.5, are plotted in Fig. 14. Superimposed on these profiles are the temperatures observed with the convective heat transfer present. The temperature profiles on Rods 2, 3, 4, and 5 are very close and similar to those given for Rods 1 and 6, hence they are not plotted in Fig. 14. Under vacuum conditions, the average temperatures on the individual rods and the outer cylinder are reproduced to within 1.2 percent of the values observed with

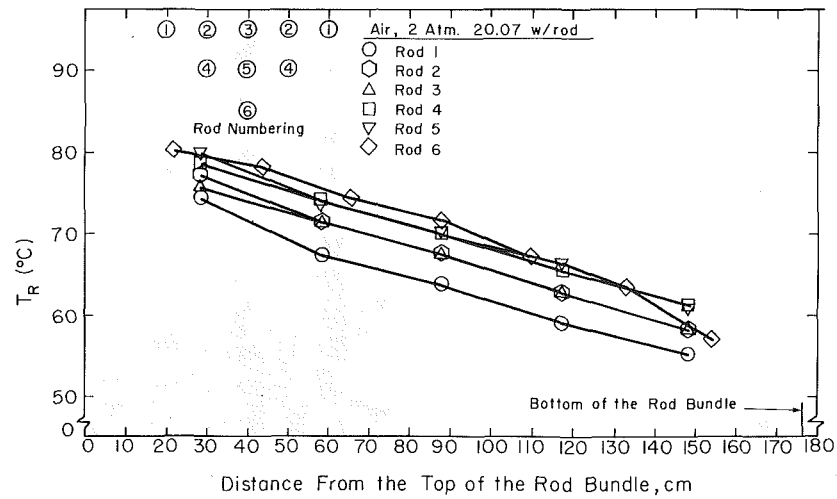

Fig. 13 Temperature profiles on Rods 1-6 at $Ra_D = 3.83 \times 10^8$

the convective effects present. However, based on absolute temperature, the difference is negligible.

The maximum radiative heat transfer contributions for Rods 1 to 6 obtained with air at atmospheric pressure at $Ra_D = 5.16 \times 10^7$, are 57, 30, 30, 25, 21, and 21 percent of the power input per rod, respectively. As the Rayleigh number is increased to 1.06×10^9 the corresponding values are reduced to, respectively, 26.5, 13.9, 13.9, 11.8, 9.8, and 9.8 percent of the power input per rod. The minimum values of the radiation heat transfer contributions for Rods 1 to 6 observed with helium at $Ra_D = 2.02 \times 10^7$ are 16.5, 8.7, 8.7, 7.5, 6.2, and 6.2 percent of the power input per rod, respectively. As can be seen from these percentages, the rods with least and most exposure to the outer cylinder, i.e., Rods 6 and 1, for a given power input per rod and test gas, have the lowest and highest heat transfer due to radiation, respectively.

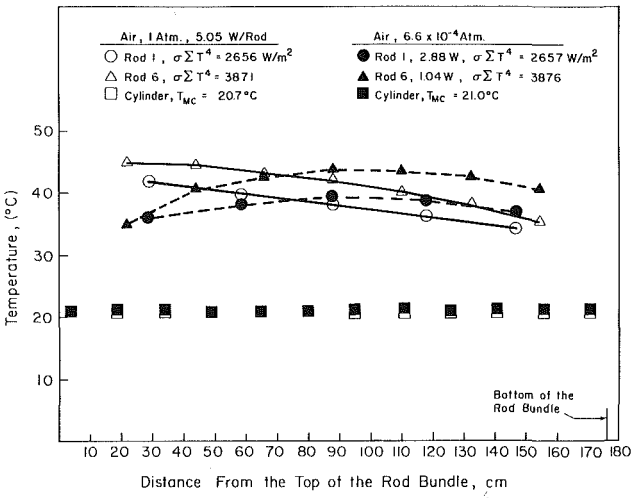

Fig. 14 Temperature profiles on Rods 1 and 6 under vacuum conditions

The convective Nusselt numbers Nu_d for Rods 1 to 6 are graphically presented as a function of Rayleigh number Ra_d in Fig. 15. As can be seen from the figure, Rods 2, 3, 4, 5, and 6, for a given Ra_d, have nearly the same heat transfer coefficient. Also, eight data points for Rod 1, out of a total of thirteen points, are within 15 percent of the values obtained for other rods. The primary reason for the scatter in the data obtained for Rod 1 is that the radial conduction heat transfer effect, present in the vacuum experiments, is most pronounced for this rod. This is due to the fact that Rod 1 is closest to the outer cylinder. Consequently, the convective heat transfer coefficients obtained for this rod are overcorrected for radiation effect. This is especially evident from the data obtained with air at pressures of 1 and 2 atm (see Fig. 15, $Ra_d = 10{,}000$ to $60{,}000$).

The convective Nusselt number for Rods 1 to 6, except five data points for Rod 1, can all be represented as a function of Ra_d through a single correlation with a maximum deviation of 12 percent. However, it is preferred to provide correlations for each rod in the array with much lower deviations from the experimental values. These correlations are as follows

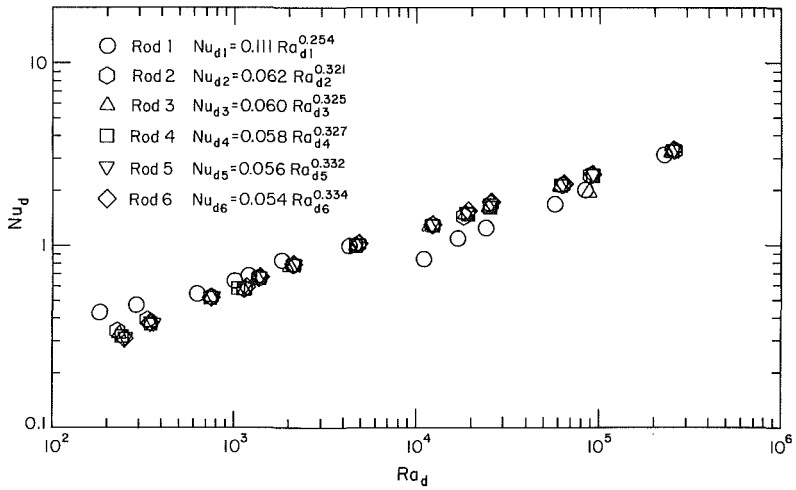

Fig. 15 Convective Nusselt numbers for the individual rods in the 5 × 5 rod bundle

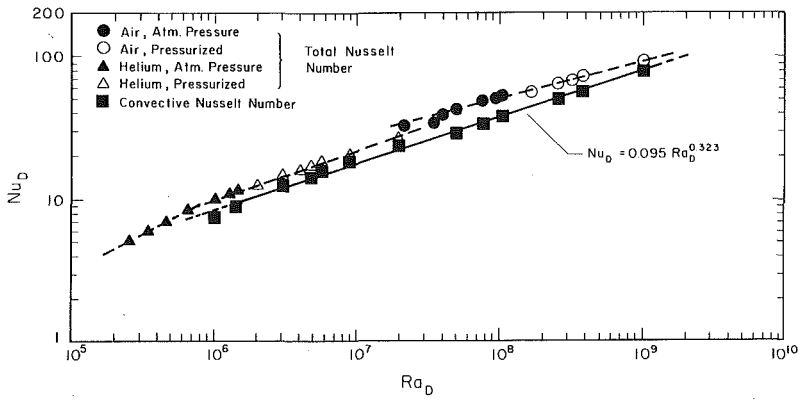

Fig. 16 Overall convective Nusselt number for the 5 × 5 rod bundle as a function of Ra_D

Table 1 Geometric parameters of the three experimental facilities

$N \times N$	d (cm)	P/d	L (cm)	D (cm)	L/D
1×1*	1.91	1	87.63	8.255	10.62
3×3	0.635	3.08	87.63	8.255	10.62
5×5	1.91	2.25	176.53	30.48	5.79

*Annulus experiments [7]

Rod 1

$$\mathrm{Nu}_{d1} = 0.111\mathrm{Ra}_{d1}^{0.254},\ 1.8 \times 10^2 \le \mathrm{Ra}_{d1} \le 2.3 \times 10^5 \quad (11)$$

Rod 2

$$\mathrm{Nu}_{d2} = 0.062\mathrm{Ra}_{d2}^{0.321},\ 2.2 \times 10^2 \le \mathrm{Ra}_{d2} \le 2.5 \times 10^5 \quad (12)$$

Rod 3

$$\mathrm{Nu}_{d3} = 0.06\mathrm{Ra}_{d3}^{0.325},\ 2.3 \times 10^2 \le \mathrm{Ra}_{d3} \le 2.5 \times 10^5 \quad (13)$$

Rod 4

$$\mathrm{Nu}_{d4} = 0.058\mathrm{Ra}_{d4}^{0.327},\ 2.4 \times 10^2 \le \mathrm{Ra}_{d4} \le 2.6 \times 10^5 \quad (14)$$

Rod 5

$$\mathrm{Nu}_{d5} = 0.056\mathrm{Ra}_{d5}^{0.332},\ 2.5 \times 10^2 \le \mathrm{Ra}_{d5} \le 2.6 \times 10^5 \quad (15)$$

Rod 6

$$\mathrm{Nu}_{d6} = 0.054\mathrm{Ra}_{d6}^{0.334},\ 2.5 \times 10^2 \le \mathrm{Ra}_{d6} \le 2.6 \times 10^5. \quad (16)$$

The above correlations, except equation (11), describe the experimental data with a maximum deviation of 6 percent. The correlation given for Rod 1, obtained through correlating all the data points for that rod, deviates from the experimental data as much as 40 percent. As mentioned before, the four data points obtained with air at 1 and 2 atm are overcorrected for the radiative heat transfer effect for this rod. If one neglects these four points the rest of the data can be correlated, with a maximum deviation of 7 percent, as

$$\mathrm{Nu}_{d1} = 0.1\mathrm{Ra}_{d1}^{0.272}. \quad (17)$$

Although the errors in some of the convective Nusselt numbers obtained for Rod 1 are very high, the effect on the overall convective Nusselt numbers Nu_D is rather small. This is due to the fact that there are only four rods out of a total of twenty-five rods numbered 1.

Overall convective and total Nusselt numbers as a function of Rayleigh number are graphically presented in Fig. 16. For air, radiation heat transfer accounts for 15–32 percent of the total power input, whereas with helium the radiation contribution is reduced to 12–23 percent. The correlation for the convective Nusselt number as a function of Rayleigh number is

$$\mathrm{Nu}_D = 0.095\mathrm{Ra}_D^{0.323},\ 1.48 \times 10^6 \le \mathrm{Ra}_D \le 1.06 \times 10^9. \quad (18)$$

Equation (18) describes the experimental data with a maximum deviation of 6 percent.

The experimental errors due to uncertainty in the measured quantities and thermophysical properties are about 5 and 8 percent for the Nusselt and Rayleigh numbers, respectively. As we discussed for the 3×3 rod bundle, the losses and the radial conduction effect in the vacuum experiments add to the uncertainty in the Nusselt number. An analysis of these effects [8] indicates that over 90 percent of the overall Nusselt numbers are underestimated by about 3.6 percent or less, with the maximum deviation not exceeding 7.4 percent for all data points. Considering the complicated geometry of the problem, the total uncertainty of about 8 to 12 percent in the overall convective Nusselt numbers is not unreasonable.

Generalized Correlation

In this section the results for an annulus [7], the 3×3 rod bundle, and the 5×5 rod bundle are brought together and analyzed. The objective is to establish an "equivalent" annulus model which can describe overall convective heat transfer from a rod bundle to its enclosing cylinder while the effects of the appropriate geometric parameters are taken into account. The geometric parameters of the three experiments are given in Table 1.

It is reasonable to state that, as far as the interior surface of a canister enclosing a rod bundle is concerned, it is receiving energy by convection, owing to a characteristic temperature difference, from the descending hot fluid. The average convective heat transfer coefficient encountered due to this heat transfer can be assumed to result from the presence of a fictitious cylinder concentric with the canister. Such an equivalent annulus should satisfy two conditions. First, the point of departure from the conduction regime should comply with the criteria set for an annulus. Second, the dependence of the effective, or overall Nusselt number on the Rayleigh number should, within the limits of experimental uncertainties, agree with those of an annulus. However, the magnitude of the Nusselt numbers for such an equivalent annulus cannot be expected to be the same as those obtained from generalized correlations for free convection in an annulus. Therefore, the pitch-to-diameter ratio and the number of rows in the bundle are expected to enter any generalized correlation for thermal convection.

Thus, in order to successfully represent thermal convection in a rod bundle with an equivalent annulus model the following tasks should be accomplished:

1 To establish the radius ratio and aspect ratio effects on heat transfer in an annulus. Furthermore, provide criteria for the extent of conduction regime as a function of the geometric parameters of H and K.

2 To identify an equivalent inner cylinder for rod bundles in such a way that the criteria for the extent of conduction regime in an annulus are satisfied.

3 To identify the effects of pitch-to-diameter ratio P/d and N, the number of rows in the square rod array, through normalizing the results for the annulus and those of rod bundles, defined based on the equivalent annulus, with respect to the H and K effects.

The annulus results of Keyhani, Kulacki, and Christensen [7] for $K = 4.33$ and $H = 27.6$, with the power law dependence of aspect and radius ratios as reported by Thomas and de Vahl Davis [13] for the conduction and boundary layer regimes are,

$$\mathrm{Nu} = 0.797\mathrm{Ra}^{0.077}H^{-0.052}K^{0.505}, \quad (19)$$

and

$$\mathrm{Nu} = 0.188\mathrm{Ra}^{0.322}H^{-0.238}K^{0.442}, \quad (20)$$

for $\mathrm{Ra} \le 2.3 \times 10^6$ and $\mathrm{Pr} = 0.71$.

It should be noted that the numerically predicted effects of radius and aspect ratios [13] have been verified through favorable agreement with the experimental results of Sheriff [16] in [7].

As for the extent of the conduction regime, Thomas and de Vahl Davis [13] have suggested the following for critical Rayleigh number:

$$\mathrm{Ra} \le 400H. \quad (21)$$

It may be noted that equation (21) does not include the radius ratio K as a parameter which influences the extent of the conduction regime. They have indicated, however, that the

Table 2 Experimental Rayleigh numbers indicating the extent of conduction regime for an annulus

	H	K	Ra_{exp}	Equation (21)	Equation (22)	$\frac{Ra_{exp}}{\text{Equation (21)}}$	$\frac{Ra_{exp}}{\text{Equation (22)}}$
Keyhani et al. [7]	2.76	4.33	6.6×10^6	1.10×10^4	6.52×10^3	1.67	0.99
Bhushan	38.38	8.28	8.79×10^3	1.54×10^4	9.85×10^3	1.74	1.12
et al. [17]	52.82	2.77	1.89×10^4	2.11×10^4	9.55×10^3	1.74	0.51
Choi and Korpela [18]	38.89	1.46	5.32×10^3	1.55×10^4	6.44×10^3	2.96	1.23

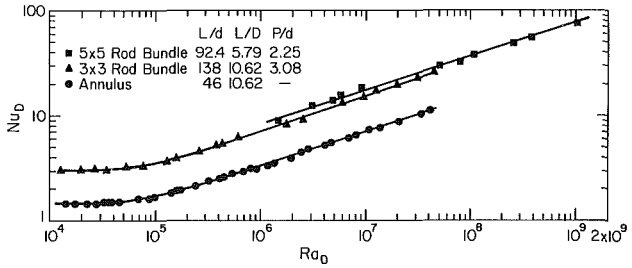

Fig. 17 Comparison of the overall convective Nusselt numbers Nu_d for the 3 × 3 and 5 × 5 rod bundles with the annulus results [7]

radius ratio has a weak effect. On the other hand, equations (19) and (20) indicate that the conduction regime is delimited by

$$Ra \leq 363 K^{0.25} H^{0.76}. \tag{22}$$

The values of the critical Rayleigh numbers for the end of the conduction regime, as predicted by equations (21) and (22), are compared with the available experimental data for annular enclosures in Table 2. The criterion given by Thomas and de Vahl Davis [13] yields a good agreement with only one piece of experimental data. The relation suggested by the present work, however, provides good agreement with three experimental values. It is felt, therefore, that equation (22) yields an acceptable value for the extent of the conduction regime.

For the annulus case, the aspect ratio and radius ratio effects and the criteria for the extent of conduction regime are experimentally established. In order to present the 3 × 3 and 5 × 5 data based on an equivalent annulus, as discussed earlier, two conditions should be met. First, the criteria for the conduction regime should be satisfied. Second, the dependence of the overall Nusselt number on the Rayleigh numbers should, within the limits of experimental uncertainties, agree with that of an annulus. The correlations obtained for the 3 × 3 and 5 × 5 rod bundles yield exponents for the Rayleigh number which are very close to that obtained for the annulus. Therefore, the second condition is adequately satisfied. As for the first condition, the conduction regime was only observed with the 3 × 3 rod bundle.

The annulus data, $K = 4.33$, $H = 27.6$, represented in terms of Ra_D and Nu_D are graphically presented along with those of 3 × 3 and 5 × 5 rod bundles in Fig. 17. As can be seen from the figure, the dependence of Nusselt number on Rayleigh number is nearly the same for the three geometries. It is only the magnitudes of the Nusselt numbers which are different. Further examination of Fig. 17 reveals that the extent of conduction regime in terms of Ra_D is nearly the same for the annulus and the 3 × 3 rod bundle. It should be mentioned here that the same outer cylinder was used for both annulus and the 3 × 3 rod bundle experiments.

Heat transfer correlations for the 3 × 3 rod bundle, equations (7) and (8), indicate that the conduction regime in that geometry is delimited by $Ra_D \leq 1.22 \times 10^5$. Furthermore, equation (22) in terms of Ra_D relates the value of the critical Rayleigh number to the geometric parameters by

$$Ra_D = 363 \left[\frac{D}{d_i}\right]^{0.25} \left[\frac{2L}{D-d_i}\right]^{0.76} \left[\frac{2D}{D-d_i}\right]^{3}, \tag{23}$$

where d_i, D, and L are diameters of the equivalent inner cylinder, diameter of the outer cylinder, and height of the cylinder or rod, respectively. With the values of Ra_D, D, and L known, one can readily solve for the diameter of the equivalent inner cylinder. It is found that a choice of inner cylinder with a diameter equal to that of a circle fitted inside the square formed by the rods as if they were close packed, i.e., $d_i = Nd$, would result in an equivalent annulus which satisfies the criteria for conduction regime, equation (23), to within 5.7 percent of the experimental value. Based on this fictitious inner cylinder, the equivalent annulus for the 3 × 3 rod bundle would have the geometric parameters of $H = 27.6$ and $K = 4.33$. Fortuitously, this equivalent annulus for the 3 × 3 rod bundle has the same aspect and radius ratios as the annulus case. The equivalent annulus for the 5 × 5 rod bundle, with $d_i = Nd$, would have the geometric parameters of $H = 16.85$ and $K = 3.2$.

With the equivalent annulus for the rod bundles selected, the experimental Nusselt and Rayleigh numbers can be calculated for such geometry. The overall convective Nusselt numbers are calculated based on the surface area of the equivalent inner cylinder. The characteristic length used in the definition of Rayleigh and Nusselt numbers would be $l = (D - Nd)/2$. In order to empirically obtain the effects of pitch-to-diameter ratio P/d and N, the number of rows in the square rod array, the experimental Nusselt numbers for the three cases can be normalized as $Nu/H^{-0.238} K^{0.442}$, where the aspect and radius ratio effects used here are the same as those reported by Thomas and de Vahl Davis for the boundary layer regime. Any difference between the three sets of normalized Nusselt numbers as a function of Rayleigh number can then be attributed to the P/d and N effects. Based on this analysis, the effects of P/d and N are empirically found as $(P/d)^{0.045N+0.541}$.

As should be expected, the effects of P/d and N are interdependent. For example, consider a close-packed 15 × 15 rod bundle, i.e., $P/d = 1$ and $N = 15$. The number of rods in this case does not have any effect on convective heat transfer other than that already included in the definition of the equivalent inner cylinder. Heat is conducted from the interior rods to the outside rods. Thereafter, the energy is transferred to the outer cylinder through combined processes of radiative and convective heat transfer. Therefore, the fact that P/d has an exponent which includes N has a physical basis. Furthermore, the constant 0.541 in the exponent of the P/d term can also be explained. Since the equivalent inner cylinder is taken as if the rod bundle were close packed, the curvature effects of the rods are not fully accounted for yet. Each curvature enhances heat transfer, and the term $(P/d)^{0.541}$ accounts for the additional curvature effect which is not incorporated into the radius ratio term.

The overall convective Nusselt numbers obtained from the 3 × 3 rod bundle experiment are calculated for the equivalent annulus of $H = 27.6$ and $K = 4.33$ and normalized as $Nu/(P/d)^{0.045N+0.541}$. These values are compared to the annulus results ($K = 4.33$, $H = 27.6$) in Fig. 18. As can be seen from the figure, the agreement between the two results is very good. It may be noted that the 3 × 3 rod bundle results defined in terms of the equivalent annulus indicate that the conduction regime ends at $Ra = 6.8 \times 10^3$, where the an-

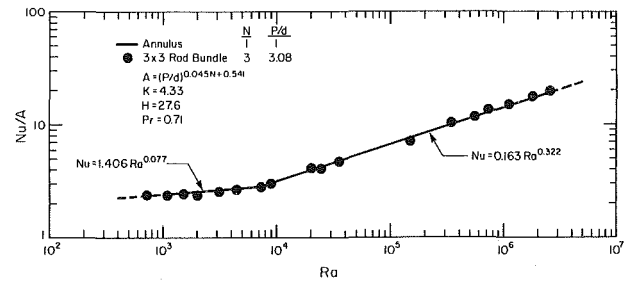

Fig. 18 Comparison of the overall convective Nusselt numbers for the 3 × 3 rod bundle, defined for the equivalent annulus, with the annulus results [7]

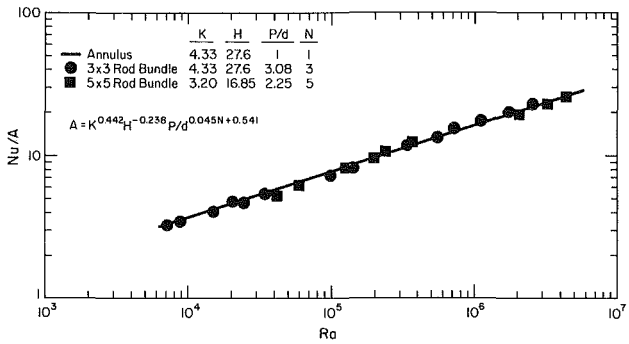

Fig. 19 The annulus [7], 3 × 3, and 5 × 5 rod bundle Nusselt numbers normalized with respect to *K*, *H*, *P/d*, and *N* effects

nulus results yield a value of Ra = 6.6×10^3. Therefore, it is felt that the appropriate equivalent inner cylinder is selected.

The annulus results and the overall convective Nusselt numbers for the 3 × 3 and 5 × 5 rod bundles defined for their respective equivalent annulus are normalized, i.e., dividing the Nusselt number for each geometry with its respective $K^{0.442}\ H^{-0.238}\ (P/d)^{0.045N+0.541}$, and graphically presented in Fig. 19 as a function of Rayleigh number. Considering the complexity of the geometries studied here, the agreement between the three sets of results is very good.

The effects of aspect ratio H, radius ratio K, pitch-to-diameter ratio P/d, and N, the number of rows in the square rod array, as selected here, lead to an adequate description of the experimental results for the annulus, 3 × 3 and 5 × 5 rod bundles. In the boundary layer regime, with the geometric effects taken as selected above, the experimental results for the three geometries can be correlated as

$$\mathrm{Nu} = 0.188K^{0.442}H^{-0.238}(P/d)^{0.045N+0.541}\mathrm{Ra}^{0.322}. \quad (24)$$

The above correlation describes over 90 percent of the data for the annulus, the 3 × 3 rod bundle, and the 5 × 5 rod bundle to within 7 percent. In the conduction regime, a correlation of the form

$$\mathrm{Nu} = 0.797K^{0.505}H^{-0.052}(P/d)^{0.045N+0.541}\mathrm{Ra}^{0.077} \quad (25)$$

describes over 90 percent of the data for the annulus and the 3 × 3 rod bundle to within 6 percent. For the 5 × 5 rod bundle, the experimental apparatus did not permit data in the conduction regime. Based on the equivalent annulus Rayleigh number, the lowest value covered is Ra = 5×10^4. Using the criteria given for the conduction regime, equation (22), conduction regime should be observed in the 5 × 5 rod bundle for Ra ≤ 4.15×10^3. It may be noted that equations (24) and (25) can readily be represented in terms of a modified Rayleigh number based on the convective heat flux rather than temperature difference, i.e., Ra* = RaNu.

Conclusions

A comparison of air and water results obtained with the 3 × 3, P/d = 3.08, rod bundle essentially confirms the Prandtl number effect found in [8] and [12] for an annulus. Therefore, it is felt that the radiation correction, as applied to the rod bundle results, is accurate. With air or helium as the convective media, different heat transfer coefficients for each rod in the array are found. The difference is most pronounced in the conduction regime and decreases with increase in Ra_d. Furthermore, the end of conduction regime data show that it is quite possible for the individual rods in the array, at a given condition, to exchange energy with the working fluid via different but coexisting flow regimes.

The water results which are obtained at high Rayleigh numbers, but overlapping the later part of air data, yield nearly the same heat transfer coefficient for the rods in the bundle. This observation may prove helpful in approximate analysis of rod bundle problems for high Rayleigh number flow. It may be noted that the 5 × 5, P/d = 2.25, rod bundle experiments with air and helium also resulted in nearly the same heat transfer coefficients for the individual rods in the array.

An equivalent annulus model for enclosed rod bundles is proposed. Based on this model, the boundary layer data obtained with air and helium from an annulus in [7], the 3 × 3 rod bundle, and the 5 × 5 rod bundle are correlated by a single equation in terms of Ra, H, K, P/d, and N. Furthermore, the conduction regime data for the annulus and the 3 × 3 rod bundle are also represented by a correlation in terms of the above parameters. In addition, the conduction regime data obtained with the 3 × 3 rod bundle, defined based on the equivalent annulus model, complies with the conduction regime criteria for an annulus (equation (22)).

It is found that, for a fixed H and K as defined for the rod bundles, an increase in the pitch-to-diameter ratio P/d, and/or N, the number of rows in the square rod array, results in an increase in the overall convective heat transfer coefficient. Moreover, for a fixed outer cylinder, an increase in P/d and/or N enhances the convective heat transfer from the rod bundle to the outer cylinder.

Acknowledgments

We gratefully acknowledge the support of this work by the Office of Nuclear Waste Isolation under Contract E512-03900 to The Ohio State University Research Foundation and the Department of Mechanical and Aerospace Engineering at the University of Delaware.

References

1 Davis, L. P., and Perona, J. L., "Development of Free Convection Axial Flow Through a Tube Bundle," *International Journal of Heat and Mass Transfer*, Vol. 16, 1973, pp. 1425–1438.

2 Cox, R. L., *Radiative Heat Transfer in Arrays of Parallel Cylinders*, Ph.D. dissertation, University of Tennessee, 1976.

3 Reilly, J. T., Chan, C. K., Edwards, D. K., and Kastenberg, W. E., "The Effects of Thermal Radiation on the Temperature Distribution in Fuel Rod Arrays," *Nuclear Engineering and Design*, Vol. 48, 1978, pp. 340–351.

4 Watson, J. S., "Heat Transfer From Spent Reactor Fuels During Shipping: A Proposed Method for Predicting Temperature Distribution in Fuel Bundles and Comparison With Experimental Data," Oak Ridge National Laboratory, ORNL-3439, May 1963.

5 Driesen, G. E., Moran, D. F., Sherba, P. S., and Steffan, R. J., "Heat Transfer Associated with Dry Storage of Spent LWR Fuel," *Heat Transfer in Nuclear Waste Disposal*, ed. F. A. Kulacki and R. Lyczkowski, HTD Vol. 11, American Society of Mechanical Engineers, 1980, pp. 9–18.

6 McCann, R., "Thermal Hydraulic Analysis of a Spent Fuel Assembly Contained Within a Canister," *Heat Transfer in Nuclear Waste Disposal*, ed. F. A. Kulacki and R. Lyczkowski, HTD Vol. 11, American Society of Mechanical Engineers, 1980.

7 Keyhani, M., Kulacki, F. A., and Christensen, R. N., "Free Convection in a Vertical Annulus With Constant Heat Flux on the Inner Wall," ASME JOURNAL OF HEAT TRANSFER, Vol. 105, 1983, pp. 454–459.

8 Keyhani, M., *Free Convection in a Vertical Annulus and Rod Bundle*, Ph.D. dissertation, Department of Mechanical Engineering, The Ohio State University, 1983.

9 Keyhani, M., Kulacki, F. A., and Christensen, R. N., "Heat Transfer

Within Spent Fuel Canisters: An Experimental Laboratory Study — Final Report," Office of Nuclear Waste Isolation, Battelle Memorial Institute, Columbus, in press.

10 Korpela, S. A., Lee, Y., and Drummond, J. E., "Heat Transfer Through a Double Pane Window," ASME JOURNAL OF HEAT TRANSFER, Vol. 104, 1982, pp. 539–544.

11 MacGregor, R. K., and Emery, A. F., "Free Convection Through Vertical Plane Layers—Moderate and High Prandtl Number Fluids," ASME JOURNAL OF HEAT TRANSFER, Vol. 91, 1969, pp. 391–403.

12 Kubair, V. G., and Simha, C. R. V., "Free Convection Heat Transfer to Mercury in Vertical Annuli," *Int. J. Heat Mass Transfer*, Vol. 25, 1982, pp. 339–407.

13 Thomas, R. W., and de Vahl Davis, G., "Natural Convection in Annular and Rectangular Cavities. A Numerical Study," *Proceedings Fourth International Heat Transfer Conference*, Paris, Vol. 4, Paper NC.2.4, Elsevier, Amsterdam, 1970.

14 Graebel, W. P., "The Influence of Prandtl Number on Free Convection in a Rectangular Cavity," *Int. J. Heat Mass Transfer*, Vol. 24, 1981, pp. 125–131.

15 Sparrow, E. M., and Gregg, J. L., "The Laminar Free Convection Heat Transfer From the Outer Surface of a Vertical Cylinder," *Transactions ASME*, Vol. 78, 1956, pp. 1823–1828.

16 Sheriff, N., "Experimental Investigations of Natural Convection in Single and Multiple Vertical Annuli With High Pressure Carbon Dioxide," *Proceedings Third International Heat Transfer Conference*, Chicago, Vol. 2, 1966, pp. 132–138.

17 Bhushan, R., Keyhani, M., Christensen, R. N., and Kulacki, F. A., "Correlations for Convective Heat Transfer in Vertical Annular Gas Layers with Constant Heat Flux on the Inner Wall," ASME JOURNAL OF HEAT TRANSFER, Vol. 105, 1983, pp. 910–912.

18 Choi, I. G., and Korpela, S. A., "Stability of the Conduction Regime of Natural Convection in a Tall Vertical Annulus," *Journal of Fluid Mechanics*, Vol. 99, 1980, pp. 725–741.